Immunotargeting of the xCT Cystine/Glutamate Antiporter Potentiates the Efficacy of HER2-Targeted Immunotherapies in Breast Cancer

Immunotargeting of the xCT cystine/glutamate antiporter potentiates the efficacy of Her2-targeted immunotherapies in breast cancer

Laura Conti[1], Elisabetta Bolli[1], Antonino Di Lorenzo[1], Valentina Franceschi[2], Francesca Macchi[2], Federica Riccardo[1], Roberto Ruiu[1], Luca Russo[2], Elena Quaglino[1], Gaetano Donofrio[2*] and Federica Cavallo[1*]

[1] Department of Molecular Biotechnology and Health Sciences, University of Torino, via Nizza 52, 10126 Torino, Italy;

[2] Department of Medical Veterinary Sciences, University of Parma, Strada del Taglio 10, 43126 Parma, Italy.

[*] These authors equally contributed

Running title: Her2 and xCT combined immunotargeting in breast cancer

Keywords: Breast Cancer, xCT, Immunotherapy, Her2, Bovine herpesvirus 4-based vectors

Additional information:

Financial support: This work was supported by grants from the Fondazione AIRC per la Ricerca sul Cancro (IG 11675 and IG 21468), Fondazione Ricerca Molinette Onlus, and by the University of Torino, Italy.

Corresponding authors:

Laura Conti

University of Torino, Department of Molecular Biotechnology and Health Sciences - Molecular Biotechnology Center, Via Nizza, 52, 10126 Torino, Italy

Phone: (+39) 011 6706458; Fax (+39) 011 236 6457; e-mail: laura.conti@unito.it

Gaetano Donofrio

Department of Medical Veterinary Sciences, University of Parma, Strada del Taglio 10, 43126 Parma, Italy

Phone: (+39) 0521 902677. Fax: (+39) 0521 032672; e-mail: gaetano.donofrio@unipr.it

Conflict of interest: the authors declare no potential conflicts of interest

Word count: 4574

Number of figures: 7

Author's contributions: L.C., E.Q., G.D. and F.C. designed the project and the experiments. L.C. and F. C. wrote the paper. L.C. performed and analyzed the majority of the experiments. E.B., A.D.L., F.R., and R.R. performed experiments. V.F., F.M. and L.R. produced and characterized the viral vectors. G.D. and F.C. coordinated and directed the study. All authors have read and approved the final version of the manuscript.

Abstract

Although the introduction of Her2-targeted therapies improved the outcome of $Her2^+$ breast cancer, many patients experience resistance and metastatic progression despite treatment. Since cancer stem cell (CSCs) play a role in this mechanism, the development of therapies combining Her2-targeting with CSC inhibition could improve the management of $Her2^+$ breast cancer. We previously demonstrated that the cystine-glutamate antiporter xCT is overexpressed in mammary CSCs and is crucial for their redox balance, self-renewal and resistance to therapies, representing a promising target for breast cancer immunotherapy.

Here, we developed a combined immunotherapy targeting Her2 and xCT using the Bovine Herpes virus (BoHV)-4 vector, a safe vaccine that can confer immunogenicity to tumor antigens. Mammary cancer-prone BALB-neuT mice, transgenic for rat Her2, were immunized with the single or combined vaccines. Anti-Her2 vaccination mostly affected primary tumor by significantly slowing down mammary cancer growth, while anti-xCT vaccination primarily prevented metastasis formation. The combination of the two vaccines exerted a complementary effect. These activities were mediated by the induction of cytotoxic T cells and of specific anti-Her2 and anti-xCT antibodies that induce antibody-dependent cell cytotoxicity and hinder cancer cell proliferation. Antibodies targeting xCT, but not those targeting Her2, directly affected viability and self-renewal of CSCs as well as cell migration, inducing the anti-metastatic effect of xCT immunotargeting.

Our findings open new perspectives in the management of $Her2^+$ breast cancer, demonstrating that CSC immunotargeting through anti-xCT vaccination, by inhibiting metastasis formation that is not directly affected by Her2 immunotargeting, synergizes with Her2-directed immunotherapy.

Introduction

Breast cancer is, together with colon and lung cancers, one of the three most frequent cancers worldwide, and the most common in women. In the last years, its prognosis has improved, thanks to the progresses achieved in its early detection and therapy. However, it still represents the second cause of cancer deaths in developed countries, and its incidence and mortality are progressively increasing in Asia, Africa and South America (1).

Roughly 20% of breast cancers worldwide show overexpression or amplification of the Her2 oncogene. Although Her2 positivity is associated with poor prognosis and poor response to standard chemotherapies, the introduction of anti-Her2 monoclonal antibodies and inhibitors has improved disease free and overall survival of $Her2^+$ breast cancer patients (2). However, most patients affected by metastatic disease display primary or secondary resistance to Her2-targeted therapies. This eventually leads to disease progression despite treatment, and advanced $Her2^+$ breast cancer remains almost incurable (3). Therefore, the development of new therapeutic approaches able to increase the efficacy of Her2-targeting drugs is urgently needed.

Breast cancer stem cells (CSCs) have been identified as one of the causes for primary resistance to Her2-targeted therapies, and their presence is a negative prognostic factor for sensitivity to the anti-Her2 monoclonal antibody Trastuzumab (4). Therefore, CSC targeting may co-operate with Her2-directed therapies and prevent the development of secondary resistance, resulting in improved patients' outcome. In the last two decades, a huge effort has been devoted to identify novel CSC molecular targets and to develop new treatments able to eradicate these cells (5,6).

We have previously demonstrated that xCT, a multipass transmembrane protein encoded by the gene SLC7A11, is overexpressed in breast CSCs and plays a key role in their self-renewal and resistance to therapy (7). xCT is the light chain of the antiporter system x_c^-, which mediates the cell uptake of cystine in exchange with glutamate. On one hand, glutamate released in the tumor microenvironment by xCT activates the suppressive function of T regulatory cells (Tregs) and promotes breast cancer

cell invasion (8,9). On the other hand, imported cystine is reduced to cysteine, the rate-limiting precursor in the synthesis of glutathione (GSH). GSH is the main intracellular anti-oxidant molecule that protects cells from ferroptosis, differentiation, autophagy, senescence and toxicity induced by xenobiotics such as chemotherapeutic drugs (10).

xCT is poorly expressed in healthy tissues while overexpressed in different tumor types, including breast cancer of different histological subtypes, where its expression is particularly increased in CSCs (7,10). Indeed, the stem cell markers CD44v and Mucin-1 interact with xCT and stabilize it at the cell membrane (11). In breast cancer, xCT is overexpressed in atypical hyperplasia and invasive ductal carcinoma of different histological subtypes (7), and is linked to poor prognosis in triple negative breast cancer patients (12). Therefore, xCT is a promising target candidate for the development of combined therapies for breast cancer.

Many authors have endorsed the pharmacological inhibition of xCT as a therapeutic strategy, and a variety of compounds have been investigated. Among them erastin (13) and the FDA-approved drugs sulfasalazine (SAS) (14) and sorafenib (13). However, erastin and SAS are insoluble under physiological conditions, have poor metabolic stability and pharmacokinetics, precluding their reliable use *in vivo*. In addition, SAS and sorafenib display low specificity for xCT, and are known for their ability to inhibit NF-kB and various kinases, respectively, and to induce important side effects (10,13,15). Therefore, new ways to specifically target xCT need to be developed for clinical use.

Since immunotherapy represents a promising strategy for cancer treatment (16), we have previously developed different vaccine platforms to specifically target xCT-expressing breast CSCs. Using these vaccines we have demonstrated that xCT immunotargeting effectively impairs cancer growth and metastatic dissemination in syngeneic transplantable mouse models of breast cancer (7,17,18).

As a proof of concept that xCT immunotargeting may ameliorate the efficacy of Her2-targeted therapies, here we develop a combined immunotherapy administering Bovine Herpes virus 4 (BoHV-

4)-based vaccines targeting Her2 (BoHV-4-Her2) and xCT (BoHV-4-xCT) in a preclinical model of $Her2^+$ mammary carcinogenesis, the BALB-neuT mice (19). BoHV-4 represents a promising vaccination strategy endowed with a high potential for clinical translatability, since it is a safe vector able to induce a strong immune response to heterologous antigens, breaking the immune tolerance towards cancer-associated antigens (17,20). Indeed, we have previously demonstrated that BoHV-4-xCT is superior to other anti-xCT vaccines in inducing a specific immune response, since it is the only vector able to break the $CD8^+$ T cell tolerance and induce xCT-specific cytotoxic T lymphocytes (7,10,17,18). We here demonstrate that the combination of Her2 and xCT-targeting synergistically impairs breast cancer progression, with anti-Her2 vaccine inducing an immune response able to hinder the growth of primary tumors, and anti-xCT immunotargeting impairing CSC survival and metastatic dissemination.

Materials and Methods

Cell and tumorsphere cultures

SKBR3 and 4T1 cells were purchased from ATCC and cultured, respectively, in McCoy's 5A Modified Medium or RPMI (ThermoFisher Scientific) with 10% FBS (Sigma-Aldrich). TUBO cells were derived from BALB-neuT primary tumors (21) and cultured in DMEM (ThermoFisher Scientific) 20% FBS (21). All cells were tested negative for mycoplasma (22). Tumorspheres were generated and maintained as in (23).

Vaccine generation and *in vivo* treatment

BoHV-4-Her2 (*alias* BoHV-4-RHuT-gD), BoHV-4-xCT and the control vector BoHV-4-ctrl (*alias* BoHV-4-A29) were generate as previously described, and $TCID_{50}$ determined by limiting dilution on BEK cells (17,20). Female BALB-neuT mice were generated and maintained at the Molecular Biotechnology Center, University of Torino, and treated in accordance with the University Ethical

Committee and European guidelines under Directive 2010/63. *In vivo* treatments were approved by the Italian Ministry of Health, authorizations N° 237/2015-PR and 500/2017-PR. Mice were vaccinated six times by intraperitoneus (i.p.) injection of 10^6 $TCID_{50}$ of BoHV-4-ctrl, BoHV-4-xCT, and/or BoHV-4-Her2 at 2-week intervals, starting from 6 weeks of age; sera were collected at week 14 and 18 (Fig. 1 B). Mice were inspected weekly and progressively growing masses with a mean diameter >1 mm were regarded as tumors. Growth was monitored until all 10 mammary glands displayed a tumor or a tumor exceeded a mean diameter of 10 mm, then mice were culled, and lungs, tumors, spleens and blood collected and processed for FACS analysis or storage. Superficial lung metastases were counted using a Zeiss SEMI DV4 Spot stereomicroscope.

FACS analysis

Tumorsphere-derived cells were incubated with sera from vaccinated mice for 5 days, then dissociated cells were stained with anti-Sca1-AlexaFluor647, anti-CD44-PE and anti-mouse CD24-PE/Cy7 or anti-human CD24-FITC (Biolegend). To measure intracellular reactive oxygen species (ROS), cells were stained with 2′,7′-dihydrochlorofluorescein diacetate (Sigma-Aldrich) (7). Apoptosis was evaluated with the AnnexinV Apoptosis Kit APC (eBioscience) (24).

To evaluate xCT expression, cells were fixed/permeabilized with BD Cytofix/Cytoperm kit and stained with anti-xCT rabbit antibody (PA1-16775, ThermoFisher) followed by FITC-anti-rabbit Ig (Dako).

To analyze peripheral Tregs, heparinized blood was incubated in erythrocytes lysis buffer (155 mM NH_4Cl, 15.8 mM Na_2CO_3, 1 mM EDTA, pH 7.3) 10 minutes R.T., treated with Fc receptor blocker (anti-CD16/CD32; BD Biosciences) and stained with anti-mouse-CD45-VioGreen (Miltenyi Biotec), CD4-PE/Cy7, GITR-PE and CD25-APC (Biolegend). Cells were washed, fixed/permeabilized and stained with anti-FoxP3-FITC (eBioscience) as in (25).

Single cell suspensions obtained from lungs and tumors were treated with Fc receptor blocker (26), and stained with the following Abs: anti-mouse CD45-VioGreen, CD3-FITC, CD4-APC/Vio770, CD8-VioBlue, PD-1-APC, CD49b-PE (Miltenyi Biotec), CD69-PE/Cy7, CD44-PE, CD24-PE/Cy7 and Sca1-AlexaFluor647 as in (17). Samples were acquired on a BD FACSVerse and analyzed with FlowJO10.5.3. tSNE analysis of immune infiltrates was run on 5 samples per group. FCS3 files were downsampled to 5000 $CD45^+$ live events, then combined into a single FCS3 file using the concatenation tool. tSNE analysis was run (perplexity, 30; iterations, 1,000), then samples were grouped according to experimental groups, and visualized in the dot plots.

ELISA

Mouse sera (1:50) were incubated on plates coated with either recombinant mouse xCT (Cloud-Clone Corp., 40 ng/well), extracellular rat or human Her2 (Sino Biological, 100 ng/well) proteins or mouse xCT extracellular loop peptides (GenScript, 1 μg/well), and binding detected with HRP-conjugated anti-mouse IgG Ab (17,20).

Cytotoxicity

1×10^4 4T1 or TUBO target cells stained with 2 μM CFSE (Molecular Probes) were cultured with splenocytes (SPC) at effector:target (E:T) ratios of 200:1, 100:1, and 50:1 for 48 h, stained with 1 μg/ml 7-Amino-ActinomycinD (7-AAD, BD Biosciences), and analyzed by FACS (17). For antibody-dependent cell-mediated cytotoxicity (ADCC), E:T incubation was performed overnight in the presence of sera from vaccinated mice (1:50). % ADCC was calculated as in (17).

Immune sera effect on tumorsphere

TUBO and SKBR3-derived P1 tumorspheres were dissociated and cultured with or without sera from immunized mice (1:50) for 5 days. Spheres were counted, then processed for FACS. To measure ferroptosis, the iron chelator deferoxamine mesylate (DFO; 50 μM, Sigma-Aldrich) was added. After 24 h, cells were stained with Annexin-V-APC kit and analyzed by FACS.

182 **Cell migration assay**

183 TUBO and SKBR3 cells were treated for 1 h at 37°C in 100 µl of serum-free medium with or without
184 sera (1:20) from vaccinated mice, then seeded (1×10^5 and 5×10^4, respectively, per well) in the top
185 chamber of 24-Transwell plates (8-µm pore size; Corning). Medium with 10% FBS was inserted in
186 bottom chambers, and cells were incubated at 37°C for 48 h. Cells on the top side of the filter were
187 detached by brushing twice with cotton tipped swab. Cells migrated on the bottom side of the filter
188 were fixed with 2.5% glutaraldehyde and stained with 0.2% crystal violet (Sigma-Aldrich). Four
189 images per well were captured with an Olympus BX41 microscope and cells counted using Fiji and
190 ImageJ softwares.

191 **MTT assay**

192 1×10^4 TUBO and SKBR3 cells were let adhere overnight in complete medium in 96-well plates. Sera
193 (1:50) were then added, and cells incubated for 24, 48 or 72 h. MTT (0.5 mg/ml) was added for 4 h at
194 37°C, then the supernatant was removed and 150 µl of dimethyl sulfoxide (Sigma Aldrich) added to
195 dissolve formazan crystals. Absorbance was measured on a 680XR microplate reader (BioRad) at
196 570 nm and 650 nm (background subtraction).

197 **Meta-analysis on patient databases**

198 For prognostic analyses, the Kaplan-Meier Plotter free software (http://kmplot.com/analysis/) (27)
199 was used. Overall, relapse free and distant metastasis free survival data were presented as Kaplan –
200 Meier plots and tested for significance using log-rank tests. Patients were stratified by expression of
201 xCT (SLC7A11). To define the cutoff between high and low expression, all percentiles between the
202 lower and upper quartiles were computed, and the best performing threshold was used as a cutoff
203 through "auto select best cutoff" function. Analysis was restricted to $Her2^+$ breast cancer samples.

204 **Statistical analysis**

205 Statistical significance was evaluated using GraphPad8 software (GraphPad Inc.). Differences in
206 tumor free mice were analyzed with Mantel-Cox log-rank test. Differences in sphere formation,
207 FACS and ELISA data, metastasis and tumor multiplicity, cell migration and survival using two-
208 tailed unpaired Student's *t*-test. Values of $P < 0.05$ were considered significant.
209
210

Results

xCT expression is linked to poor prognosis in Her2$^+$ breast cancer patients

High levels of xCT expression are linked to poor prognosis in triple negative breast cancer patients (12). To analyze if the same was true for Her2$^+$ breast cancer, we ran a meta-analysis on a set of publicly available microarray data from breast cancer patients (http://kmplot.com/analysis/) (27). Patients with high levels of xCT displayed a significantly lower overall and relapse-free survival as compared to patients displaying low levels of xCT expression (Fig. 1A, B), and a trend of decrease in distant metastasis-free survival (Fig. 1C). These results suggest that xCT plays a role in breast cancer progression, relapse and metastatic spreading, and prompted us to test whether its targeting may improve the outcome of anti-Her2 immunotherapies.

xCT immunotargeting potentiates the effectiveness of anti-Her2 vaccination

We have previously demonstrated that BoHV-4-xCT impairs breast CSCs and efficiently protects mice from cancer metastases in transplantable mammary cancer models (17). We therefore hypothesized that this vaccine may improve the outcome of Her2-targeted immunotherapies. To test this hypothesis, we selected the BALB-neuT mouse model, whose rat Her2/neu$^+$ mammary tumors express xCT (Fig. 1D). BoHV-4-Her2, coding for a chimeric rat/human Her2, was used as Her2-targeting immunotherapy, since we previously demonstrated that it can break BALB-neuT immune tolerance to Her2 (20). Female BALB-neuT mice were immunized by i.p. injections of 10^6 $TCID_{50}$ of BoHV-4-xCT, BoHV-4-Her2 and control vector (BoHV-4-ctrl), alone or in combination. All mice received 6 immunizations. Each vaccine was administered 4 times, and vaccination was performed every 2 weeks (Fig. 1E). Preliminary data showed that xCT expression is higher in 6 week-old BALB-neuT mammary glands than in tumors at later stages (Supplementary Fig. S1). Furthermore, xCT is a key player both in the synthesis of GSH, which is necessary for cancer initiation but dispensable for its subsequent growth (28), and in the maintenance of CSCs, which are involved in tumor onset

(5). For these reasons, xCT immunotargeting was started in the early stages of tumor development (week 6), while Her2 immunotargeting was started at week 10, as previously reported (20).

All vaccinated mice showed a significantly longer tumor-free survival (Fig. 1F) and a slower increase in tumor multiplicity than control mice (Fig. 1G). This effect was more pronounced in mice vaccinated with Her2, alone or in combination with xCT. Of note, xCT immunotargeting protected BALB-neuT mice from the development of lung metastases (Fig. 1H). Indeed, while all control and Her2 vaccinated mice displayed lung metastases, these were observed only in 50% and 54.5% of in mice vaccinated with Her2 + xCT or xCT alone, respectively. (Fig. 1H). Moreover, the number of lung metastases was significantly reduced by anti-xCT vaccination, alone or combined with Her2 (Fig. 1I). Overall, these results demonstrate that xCT immunotargeting potentiates the effectiveness of anti-Her2 immunization by significantly hindering the development of metastases.

xCT immunotargeting decreases CSC frequency in the tumors and lungs affected by metastases

Since CSCs contribute to metastatic dissemination (5), we assessed the frequency of $Sca1^+$ and $CD44^+$ $CD24^-$ mammary CSCs in tumors and lungs from control and immunized mice. $Sca1^+$ CSCs (29) were detected in both tumors and lungs of control mice. While their frequency was not reduced by anti-Her2 vaccination, it resulted significantly reduced by xCT immunotargeting, alone or combined with anti-Her2 vaccination (Fig. 2A, B). A different scenario was observed for the $CD44^+$ $CD24^-$ CSC population, endowed with mesenchymal-like properties (30). A lower percentage of $CD44^+$ $CD24^-$ CSCs was observed in the tumors of control and vaccinated mice as compared to the lungs (Fig. 2C, D). Moreover, while in the tumors no changes in the percentages of these cells were observed in vaccinated animals independently from the vaccine used (Fig. 2C), a strong decrease of $CD44^+$ $CD24^-$ cells was observed in the lungs from mice vaccinated with Her2, xCT or both (Fig. 2D). These results confirm that xCT immunotargeting decreases CSC frequency and suggest a different sensitivity of the various CSC populations to Her2 targeting.

Her2 and xCT combined immunotargeting activates tumor infiltrating T lymphocytes

To characterize the immune mechanisms that mediate the anti-tumor and anti-metastatic potential of anti-Her2 and anti-xCT combined immunotherapies, the immune cell infiltrate in the tumors and lungs of vaccinated mice was analyzed. None of the vaccines significantly increased the percentages of tumor infiltrating NK, NKT, and $CD4^+$ T lymphocytes as compared to controls (Fig. 3A. B). However, all vaccines induced a significant increase in tumor infiltrating $CD8^+$ T cells (black population in tSNE plots), which was more enhanced in mice vaccinated with Her2 + xCT (Fig. 3A, B). Moreover, all vaccines induced T cell activation in the tumors, as suggested by the significant increase in $CD69^+$ cells in the total $CD3^+$ T cell population. Of note, the combination of Her2 and xCT immunotargeting significantly increased T cell activation as compared to anti-Her2 vaccine alone. Activation was observed in both $CD4^+$ (violet population in tSNE plots), and $CD8^+$ (blue population in tSNE plots) T cells. Moreover, anti-xCT immunotargeting induced the activation of NK cells (Fig. 3A, C). On the contrary, the expression of PD-1 in NK and T cells was not significantly altered by any vaccine, although a trend of decrease in $PD1^+$ $CD4^+$ T cells (yellow population in tSNE plot) was observed in mice vaccinated with Her2 + xCT or xCT alone (Fig. 3A, D).

None of the vaccines altered the frequency of NK, NKT or $CD4^+$ T cells in lungs, while the combination of Her2 and xCT immunotargeting induced a significant increase in $CD8^+$ T lymphocytes (Fig. 3E, F). All vaccination strategies induced the activation of NK, total $CD3^+$ T and $CD4^+$ T cells (violet population in tSNE plots), while $CD8^+$ T cells were activated only by xCT immunotargeting, alone or in combination with anti-Her2 vaccination (Fig. 3E, G; blue population in tSNE plots). As for primary tumors, the treatments did not induce significant variations in the amount of $PD\text{-}1^+$ NK or T cells (Fig. 3E, H).

Overall, these data indicate that all the vaccines induce the activation of NK and $CD4^+$ T cells in primary tumors and lungs, and of tumor-infiltrating $CD8^+$ T lymphocytes, but xCT immunotargeting is the only one able to increase the frequency and the activation of $CD8^+$ T lymphocytes in the lungs, suggesting a possible explanation for its anti-metastatic activity.

Anti-xCT vaccination induces xCT$^+$ breast cancer cell cytotoxicity and decreases circulating Tregs

To assess whether anti-Her2 and anti-xCT vaccination generates T lymphocytes able to kill breast cancer cells expressing Her2 and/or xCT antigens, we performed an *in vitro* cytotoxicity assay. SPC from the various groups were incubated with rat Her2$^+$ TUBO, or triple negative 4T1 mammary cancer cells, at different E:T ratios. Both TUBO and 4T1 cells express xCT (Supplementary Fig. S2), while only TUBO cells express Her2. In accordance with the lack of high avidity Her2-specific CD8$^+$ T cell clones in BALB-neuT mice due to central tolerance (31), SPC from Her2-vaccinated mice did not induce a significant cytotoxicity on TUBO cells and, as expected, on control 4T1 cells (Fig. 4A). On the contrary, anti-xCT vaccination induced a significant cytotoxicity of both cell lines, as previously observed in BALB/c mice (17). This effect was maintained when anti-xCT was associated with anti-Her2 vaccination (Fig. 4A), and was accompanied by a reduction of circulating Tregs, as compared to control mice (Fig. 4B).

Her2 and xCT immunotargeting induces a specific antibody response that mediates ADCC

The presence of Her2- and xCT-specific antibodies in the sera of mice two weeks after the last vaccination (18-week-old mice) was evaluated. Anti-xCT immunization induced the production of anti-xCT antibodies that were barely detectable in the sera from control and Her2-vaccinated mice (Fig. 5A). Of note, these antibodies were able to bind the xCT extracellular loops (Fig. 5B-F), suggesting that they can play a therapeutic role *in vivo* by directly binding to xCT on cancer cell surface. No differences were observed in the antibody titers between mice vaccinated with xCT alone or in combination with Her2, demonstrating that Her2 immunotargeting did not affect the response to xCT (Fig. 5A-F). Likewise, Her2 immunotargeting using the rat/human chimeric construct induced the generation of antibodies able to bind both the rat and human Her2 proteins (Fig. 5G, H). Surprisingly, anti-rat and human Her2 antibodies (Fig. 5G, H) were abundantly detected in the sera of mice vaccinated with xCT alone as well, suggesting that xCT immunotargeting in BALB-neuT

mice may induce immunogenic cancer cell death and epitope spreading. Similar results were obtained analyzing sera collected from 14-week-old mice (Supplementary Fig. S3). While the few anti-xCT antibodies present in control mice sera mainly belonged to the IgG1 isotype, vaccination induced the expansion of specific IgG2a antibodies (Fig. 5I). Similarly, the proportion of anti-Her2 IgG2a was increased by anti-Her2 vaccination as compared to control mice, with a concomitant reduction of the percentage of IgM and IgG3 (Fig. 5L). As IgG2a are the main responsible for ADCC in mice, vaccine-induced anti-Her2 and anti-xCT antibodies were able to mediate ADCC of tumor cells by SPC from syngeneic mice. As expected, sera from Her2-immunized mice induced ADCC of TUBO but not of 4T1 cells, while sera from xCT-vaccinated mice mediated ADCC of both cell lines. Of note, the combination of Her2 and xCT immunotargeting gave the best results on TUBO cells, since sera from mice vaccinated with Her2 + xCT induced a significantly higher ADCC than sera from mice treated with the single vaccines (Fig. 5M, N).

Anti-Her2 and anti-xCT antibodies differentially impair cancer cell viability and migration

Given that both anti-Her2 and anti-xCT vaccination induced a strong specific antibody response, we evaluated the direct effect that sera from vaccinated mice may exert on mammary cancer cells. TUBO cell viability was decreased after 48 and 72 h of incubation with sera from all groups of vaccinated mice, as compared to sera from control mice (Fig. 6A). To verify the possible translatability of this approach, sera were incubated with $Her2^{+}$ human breast cancer SKBR3 cells, which express xCT (Supplementary Fig. S2). SKBR3 viability was impaired at a similar extent by incubation with the sera from Her2, Her2 + xCT and xCT vaccinated mice (Fig. 6B). These data demonstrate that vaccination induces antibodies that exert a direct impairment of cancer cell viability, contributing to the therapeutic effects observed *in vivo*.

Since metastatic spreading was decreased in mice vaccinated with xCT, alone or in combination with Her2, the ability of vaccine-induced antibodies to inhibit cancer cell migration was assessed by transwell assays. As shown in Fig. 6C, sera from xCT or Her2 + xCT immunized mice significantly

impaired the migration of both $Her2^+$ murine TUBO and human SKBR3 cells *in vitro*, as confirmed by the decreased number of migrating cells (Fig. 6D, F) and area covered by migrated cells (Fig. 6E, G). No effect was exerted by sera of mice vaccinated with Her2 alone (Fig. 6C-G), indicating that xCT and Her2 immunotargeting act with different mechanisms in hampering breast cancer progression, and supporting the anti-metastatic role exerted by xCT immunotargeting *in vivo*.

Vaccine-induced xCT targeting antibodies halt CSCs increasing their ROS content, apoptosis and ferroptosis

To further investigate the mechanisms underlying the different effects induced by anti-Her2 and anti-xCT immunization on primary cancer growth and metastasis, we evaluated the ability of sera from immunized mice to target CSCs, which are considered as the main responsible for metastatic spreading. Cells derived from TUBO and SKBR3 CSC-enriched tumorspheres (23) were incubated with the sera. Sera from control mice did not alter second-generation tumorsphere formation, which was decreased by sera from Her2-vaccinated mice. A greater impairment of tumorsphere generation was induced by sera from xCT vaccinated mice and, even more, by sera from mice vaccinated with Her2 + xCT (Fig. 7A, B). This decreased CSC self-renewal potential in cells treated with sera from Her2 + xCT and xCT vaccinated mice was accompanied by a reduction in cells expressing the TUBO CSC marker $Sca1^+$ (32) (Fig. 7C). Similar results were obtained in SKBR3 tumorspheres, where sera from Her2 and, even more, from Her2 + xCT or xCT immunized mice significantly reduced the ratio between the percentage of $CD44^+$ and $CD24^+$ cells (Fig. 7D), which correlates with stemness in this cell line (33). Since xCT plays a key role in the maintenance of CSC redox balance (10), intracellular ROS content was evaluated. While ROS content of either TUBO or SKBR3 tumorspheres was not altered by control or Her2-vaccinated mice sera, ROS were significantly increased in tumorspheres treated with sera from mice vaccinated against Her2 + xCT or xCT alone (Fig. 7E and F). Moreover, these sera were able to induce apoptosis in CSCs from both cell lines, while sera from control or Her2-immunized mice had no effect (Fig. 7G, H). Sera from Her2 + xCT- or xCT-vaccinated mice

were also able to induce ferroptosis in both TUBO and SKBR3 CSCs, as demonstrated by the ability of the iron chelating agent deferoxamine (DFO) of rescuing cells from the cytotoxic effect induced by these sera. On the contrary, sera from control or Her2-vaccinated mice did not induce cell death either in the absence or presence of DFO (Fig. 7I, L).

Overall, these data demonstrate that anti-xCT vaccination is more effective than Her2 immunotargeting in reducing the CSC population, making their combination of great interest for breast cancer treatment.

Discussion

The introduction of Her2-targeted therapies in the clinical practice has significantly improved the outcome of $Her2^+$ breast cancer patients. However, most patients display primary resistance or relapse after treatment, and metastatic breast cancer is considered incurable with current therapies (34). Therefore, the setup of combined therapeutic protocols able to target the mechanisms and cell populations involved in the resistance to Her2-targeted therapies and prevent metastatic spreading is urgently needed to improve treatment efficacy. Therapies able to eradicate CSCs, which are implied in the resistance to most current therapies, including Her2-targeted therapies (4,5), may thus synergize with Her2-directed drugs and reinstate cancer sensitivity to treatment.

To this end, we have developed a combined vaccination approach targeting both Her2 and the CSC-associated antigen xCT, using BoHV-4-based viral vectors. We tested this immunotherapy in BALB-neuT mice, which represent an ideal model to study new therapies for $Her2^+$ breast cancer in virtue of the high homology of their tumors to the human counterpart (19) and of the fact that their tumors contain cells that can disseminate to the bone marrow early after the activation of Her2 transcription, and then move to the lungs where they give rise to overt metastasis (35,36).

Her2 and xCT represent self-antigens in BALB-neuT mice. Nevertheless, BoHV-4-based vaccination was able to induce a strong and specific immune response to both of them. As expected, Her2 immunotargeting induced mainly a humoral response, along with the activation of NK and T helper cells in both primary tumors and lung metastases. However, no increase of activation was observed in lung-infiltrating $CD8^+$ T lymphocytes. On the contrary, anti-xCT vaccination was able to induce both a polyclonal antibody response and the activation of tumor- and lung-infiltrating NK, $CD4^+$ and $CD8^+$ T cells. In accordance to this pattern of immune response, anti-xCT but not anti-Her2 vaccination induced cytotoxic T cells able to kill breast cancer cells. The lack of Her2-directed cytotoxicity is due to the thymic deletion of high avidity Her2-specific $CD8^+$ T cell clones in BALB-neuT mice (31). A $CD4^+$ T cell repertoire is instead generated and escapes central tolerance (31), thus allowing the induction of an anti-Her2 antibody response that is necessary for protection from autochthonous tumor development (19,20,37). BoHV-4-based anti-xCT vaccination, instead, is able to break immune tolerance and induce a T cytotoxic response, which we previously demonstrated to exert a key role *in vivo* in transplantable models of mammary cancer (17). While naive T lymphocytes lack xCT and rely on the uptake of cysteine released from antigen presenting cells for the synthesis of GSH, xCT expression is induced on T lymphocytes upon activation and is necessary for their proliferation *in vitro* (38). However, *in vivo* compensative mechanisms make xCT dispensable for T cell proliferation and anti-tumoral responses (39), allowing the induction of T cell responses in xCT-vaccinated mice. Of note, the induction of xCT-specific cytotoxic T cells is exclusive of BoHV-4-based vaccine, since neither DNA nor Virus-like particle-based vaccines exert the same effect (7,18), indicating that this vaccine formulation is superior in breaking immune tolerance to self-antigens. This is likely due to viral vectors' intrinsic immunogenicity, which creates an inflammatory environment that potentiates T lymphocyte activation (40). Moreover, xCT immunotargeting decreased Tregs frequency. This may be due to the reduction in glutamate export from xCT expressing cells, which would prevent the proliferative effect exerted by metabotropic glutamate

receptor 1 on Tregs (8), although further studies are needed to evaluate possible direct effects of xCT targeting on this cell population.

Her2 and xCT immunotargeting induced a strong antibody response. Of note, anti-xCT vaccination induced epitope spreading, with the production of antibodies able to recognize rat Her2 and react with human Her2. A similar phenomenon was previously observed using a DNA vaccine coding for the extracellular and transmembrane domain of rat Her2, which was able to induce an early spread of the immune response to Her2 intracellular epitopes (31) and antibodies able to recognize human Her2 (37). Vaccine-induced antibodies exerted both direct and indirect effects on cancer cells, inducing ADCC and directly affecting their viability. The induction of an antibody response is particularly important for the elimination of CSCs, which downregulate MHC class I and become therefore less sensitive to T cell killing (32). Indeed, sera from vaccinated mice, and in particular from mice vaccinated with xCT alone or in combination with Her2, strongly inhibited CSC self-renewal *in vitro* and altered their redox balance, inducing ROS accumulation and ferroptosis.

Anti-Her2 immunotargeting was effective in inhibiting primary tumor growth, with limited effects on metastasis. Instead, anti-xCT vaccination strongly impaired CSC self-renewal, decreased cancer cell survival and migration, thus preventing metastasis formation. Although the complex mechanisms underpinning cancer metastasis formation have not been completely dissected, recent data showed that metastatic dissemination often occurs during the early phases of cancer progression, when the frequency of CSCs in primary lesions is higher than in more advanced tumors (35). In transgenic $Her2^{+}$ mammary cancer mouse models, 80% of metastases derive from early disseminated cancer cells, which display moderate levels of Her2 and high progesterone receptor expression. These cells possess CSC features, such as Wnt pathway activation, inhibition of p38 activation and of E-cadherin- and β-catenin-mediated junction formation, thus allowing for an epithelial-to-mesenchymal transition (EMT)-like invasive program (35,41). Of note, by decreasing intracellular ROS content, xCT inhibits p38 activation, thus diminishing caveolin-1 and the subsequent recruitment of β-catenin to the plasma

membrane, suggesting that xCT may contribute to the invasive properties of disseminating cells (42). Indeed, we have preliminary data showing that early disseminated cancer cells present in the bone marrow of 7-week-old BALB-neuT mice express xCT. Therefore, xCT immunotargeting may hinder metastasis formation by inducing the eradication of early disseminated cancer cells and CSCs that are responsible for tumor spreading to distal organs. On the contrary, Her2 expression is low in early lesions and in early disseminated cancer cells, while it increases during cancer growth, and Her2 activation seems to be more involved in the proliferation of disseminated cells than in their migration (35). Moreover, despite several reports indicating that Her2 promotes breast CSC self-renewal (43), different groups have demonstrated that Her2 inhibition leads to Notch1 activation, thus promoting CSC expansion and tumor recurrence and metastasis (44,45). Indeed, CSCs from SKBR3 cells are resistant to Her2-targeted therapies (46), in accordance with our data showing that antibodies from Her2-vaccinated mice exert only a mild inhibitory effect on SKBR3 tumorspheres, which are effectively inhibited by antibodies from xCT-vaccinated mice. Overall, our data and evidences from the literature suggest that Her2 and xCT immunotargeting may act synergistically, with anti-Her2 immune response mainly affecting cancer growth, and anti-xCT immune reaction hindering metastatic spreading.

While Her2-directed immunotherapy are currently used in the clinical practice, the clinical translatability of xCT immunotargeting may be questioned by its nature of cancer-associated antigen also expressed on astrocytes, some myeloid cell types and activated T cells (10). However, the safety of xCT targeting is supported by the lack of organ alterations, developmental and immunological defects in xCT knockout mice (39,47) and in Subtle grey mice harboring a spontaneous protein null mutation in the xCT allele (48). Indeed, the xCT inhibitor SAS is widely used for the treatment of inflammatory diseases such as Crohn's disease and ulcerative colitis (49). Moreover, no adverse events were observed here in xCT-vaccinated BALB-neuT mice or previously in xCT-vaccinated BALB/c mice (7,17), and no alterations or immune infiltration were observed in the central nervous

system of mice vaccinated with xCT-targeting virus-like particles (18). Therefore, the possibility of targeting xCT for cancer treatment has recently attracted the attention of pharmaceutical companies (39).

The recent clinical successes of checkpoint blocking antibodies and of chimeric antigen receptor T cells has opened a new golden age for cancer immunotherapy, leading many researchers to focus on these new immunotherapies. However, we believe that vaccination still represents a promising approach, since the activation of antigen-specific anti-tumor responses may effectively hamper cancer progression (3). In this article, we chose to target both Her2 and xCT with vaccination. Although we think that anti-xCT vaccination can improve the effectiveness of any of the current Her2-targeted therapies, and we are conscious that monoclonal antibodies and molecular inhibitors currently play a major role in Her2-targeted therapies, we think that anti-Her2 vaccination should still be kept in high consideration for cancer treatment. Indeed, vaccination is a cost-effective strategy as compared to more expensive monoclonal antibodies and lymphocyte adoptive therapies. Breast cancer incidence is rapidly increasing in low- and middle-income countries, where the lack of resources and investments makes breast cancer a neglected disease, causing high mortality rates and health inequity (1). The development of effective anti-Her2 vaccines might provide more affordable and accessible therapies able to improve life expectancy of hundreds of thousands of women that currently have to face disability and premature death from breast cancer. In this view, BoHV-4 represents a promising vector in virtue of its absence of pathogenicity or oncogenic activity, the possibility of performing repeated boosts without inducing virus neutralizing antibodies, and its ability to induce a strong immune response able to break tolerance to cancer-associated antigens (50).

In conclusion, our findings demonstrate that xCT immunotargeting synergizes with Her2-directed immunotherapy in hampering breast cancer progression and metastasis. Indeed, while Her2 immunotargeting mainly impairs the growth of primary tumor, anti-xCT vaccination strongly affects CSCs and inhibits the generation of lung metastases. This combinatorial immunotherapeutic approach

483 could be combined with treatments such as immune checkpoint inhibitors or chemotherapy to further
484 induce anti-cancer immune responses, opening new perspectives in the management of $Her2^{+}$ breast
485 cancer.

486

487 **Acknowledgments:** we thank Dr. Irene Merighi for breeding and genotyping the mice.

488

References

1. Ginsburg O, Bray F, Coleman MP, Vanderpuye V, Eniu A, Kotha SR*, et al.* The global burden of women's cancers: a grand challenge in global health. Lancet **2017**;389(10071):847-60 doi 10.1016/S0140-6736(16)31392-7.
2. Wang J, Xu B. Targeted therapeutic options and future perspectives for HER2-positive breast cancer. Signal transduction and targeted therapy **2019**;4:34 doi 10.1038/s41392-019-0069-2.
3. Krasniqi E, Barchiesi G, Pizzuti L, Mazzotta M, Venuti A, Maugeri-Sacca M*, et al.* Immunotherapy in HER2-positive breast cancer: state of the art and future perspectives. J Hematol Oncol **2019**;12(1):111 doi 10.1186/s13045-019-0798-2.
4. Seo AN, Lee HJ, Kim EJ, Jang MH, Kim YJ, Kim JH*, et al.* Expression of breast cancer stem cell markers as predictors of prognosis and response to trastuzumab in HER2-positive breast cancer. Br J Cancer **2016**;114(10):1109-16 doi 10.1038/bjc.2016.101.
5. Ruiu R, Tarone L, Rolih V, Barutello G, Bolli E, Riccardo F*, et al.* Cancer stem cell immunology and immunotherapy: Harnessing the immune system against cancer's source. Progress in molecular biology and translational science **2019**;164:119-88 doi 10.1016/bs.pmbts.2019.03.008.
6. Quaglino EC, L.; Cavallo, F. Breast cancer stem cell antigens as targets for immunotherapy. Seminars in immunology **2020** doi 10.1016/j.smim.2020.101386.
7. Lanzardo S, Conti L, Rooke R, Ruiu R, Accart N, Bolli E*, et al.* Immunotargeting of Antigen xCT Attenuates Stem-like Cell Behavior and Metastatic Progression in Breast Cancer. Cancer Res **2016**;76(1):62-72 doi 0008-5472.CAN-15-1208 [pii]

10.1158/0008-5472.CAN-15-1208.

8. Long Y, Tao H, Karachi A, Grippin AJ, Jin L, Chang YE*, et al.* Dysregulation of glutamate transport enhances Treg function that promotes VEGF blockade resistance in glioblastoma. Cancer Res **2019** doi 10.1158/0008-5472.CAN-19-1577.
9. Dornier E, Rabas N, Mitchell L, Novo D, Dhayade S, Marco S*, et al.* Glutaminolysis drives membrane trafficking to promote invasiveness of breast cancer cells. Nature communications **2017**;8(1):2255 doi 10.1038/s41467-017-02101-2.
10. Ruiu R, Rolih V, Bolli E, Barutello G, Riccardo F, Quaglino E*, et al.* Fighting breast cancer stem cells through the immune-targeting of the xCT cystine-glutamate antiporter. Cancer Immunol Immunother **2018**;68(1):131-41 doi 10.1007/s00262-018-2185-1.

11. Hasegawa M, Takahashi H, Rajabi H, Alam M, Suzuki Y, Yin L*, et al.* Functional interactions of the cystine/glutamate antiporter, CD44v and MUC1-C oncoprotein in triple-negative breast cancer cells. Oncotarget **2016**;7(11):11756-69 doi 10.18632/oncotarget.7598.
12. Briggs KJ, Koivunen P, Cao S, Backus KM, Olenchock BA, Patel H*, et al.* Paracrine Induction of HIF by Glutamate in Breast Cancer: EglN1 Senses Cysteine. Cell **2016**;166(1):126-39 doi 10.1016/j.cell.2016.05.042.
13. Dixon SJ, Patel DN, Welsch M, Skouta R, Lee ED, Hayano M*, et al.* Pharmacological inhibition of cystine-glutamate exchange induces endoplasmic reticulum stress and ferroptosis. eLife **2014**;3:e02523 doi 10.7554/eLife.02523.
14. Linares V, Alonso V, Domingo JL. Oxidative stress as a mechanism underlying sulfasalazine-induced toxicity. Expert Opin Drug Saf **2011**;10(2):253-63 doi 10.1517/14740338.2011.529898.
15. Robe PA, Martin DH, Nguyen-Khac MT, Artesi M, Deprez M, Albert A*, et al.* Early termination of ISRCTN45828668, a phase 1/2 prospective, randomized study of sulfasalazine for the treatment of progressing malignant gliomas in adults. BMC cancer **2009**;9:372 doi 10.1186/1471-2407-9-372.
16. Dillman RO. Is there a role for therapeutic cancer vaccines in the age of checkpoint inhibitors? Human vaccines & immunotherapeutics **2017**;13(3):528-32 doi 10.1080/21645515.2016.1244149.
17. Donofrio G, Tebaldi G, Lanzardo S, Ruiu R, Bolli E, Ballatore A*, et al.* Bovine herpesvirus 4-based vector delivering the full length xCT DNA efficiently protects mice from mammary cancer metastases by targeting cancer stem cells. Oncoimmunology **2018**;7(12):e1494108 doi 10.1080/2162402X.2018.1494108.
18. Bolli E, O'Rourke JP, Conti L, Lanzardo S, Rolih V, Christen JM*, et al.* A Virus-Like-Particle immunotherapy targeting Epitope-Specific anti-xCT expressed on cancer stem cell inhibits the progression of metastatic cancer in vivo. Oncoimmunology **2017**:e1408746 doi 10.1080/2162402X.2017.1408746.
19. Conti L, Ruiu R, Barutello G, Macagno M, Bandini S, Cavallo F*, et al.* Microenvironment, oncoantigens, and antitumor vaccination: lessons learned from BALB-neuT mice. Biomed Res Int **2014**;2014:534969 doi 10.1155/2014/534969.
20. Jacca S, Rolih V, Quaglino E, Franceschi V, Tebaldi G, Bolli E*, et al.* Bovine herpesvirus 4-based vector delivering a hybrid rat/human HER-2 oncoantigen efficiently protects mice from autochthonous Her-2(+) mammary cancer. Oncoimmunology **2016**;5(3):e1082705 doi 10.1080/2162402X.2015.1082705.

21. Rovero S, Amici A, Di Carlo E, Bei R, Nanni P, Quaglino E*, et al.* DNA vaccination against rat her-2/Neu p185 more effectively inhibits carcinogenesis than transplantable carcinomas in transgenic BALB/c mice. J Immunol **2000**;165(9):5133-42 doi 10.4049/jimmunol.165.9.5133
22. Geninatti Crich S, Cadenazzi M, Lanzardo S, Conti L, Ruiu R, Alberti D*, et al.* Targeting ferritin receptors for the selective delivery of imaging and therapeutic agents to breast cancer cells. Nanoscale **2015**;7(15):6527-33 doi 10.1039/c5nr00352k.
23. Conti L, Lanzardo S, Arigoni M, Antonazzo R, Radaelli E, Cantarella D*, et al.* The noninflammatory role of high mobility group box 1/Toll-like receptor 2 axis in the self-renewal of mammary cancer stem cells. FASEB J **2013**;27(12):4731-44 doi 10.1096/fj.13-230201.
24. Regis G, Icardi L, Conti L, Chiarle R, Piva R, Giovarelli M*, et al.* IL-6, but not IFN-gamma, triggers apoptosis and inhibits in vivo growth of human malignant T cells on STAT3 silencing. Leukemia **2009**;23(11):2102-8 doi 10.1038/leu.2009.139.
25. Bandini S, Macagno M, Hysi A, Lanzardo S, Conti L, Bello A*, et al.* The non-inflammatory role of C1q during Her2/neu-driven mammary carcinogenesis. Oncoimmunology **2016**;5(12):e1253653 doi 10.1080/2162402X.2016.1253653.
26. Macagno M, Bandini S, Stramucci L, Quaglino E, Conti L, Balmas E*, et al.* Multiple roles of perforin in hampering ERBB-2 (Her-2/neu) carcinogenesis in transgenic male mice. J Immunol **2014**;192(11):5434-41 doi 10.4049/jimmunol.1301248.
27. Győrffy B, Lanczky A, Eklund AC, Denkert C, Budczies J, Li Q*, et al.* An online survival analysis tool to rapidly assess the effect of 22,277 genes on breast cancer prognosis using microarray data of 1,809 patients. Breast cancer research and treatment **2010**;123:725-31 doi 10.1007/s10549-009-0674-9.
28. Harris IS, Treloar AE, Inoue S, Sasaki M, Gorrini C, Lee KC*, et al.* Glutathione and thioredoxin antioxidant pathways synergize to drive cancer initiation and progression. Cancer cell **2015**;27(2):211-22 doi 10.1016/j.ccell.2014.11.019.
29. Grange C, Lanzardo S, Cavallo F, Camussi G, Bussolati B. Sca-1 identifies the tumor-initiating cells in mammary tumors of BALB-neuT transgenic mice. Neoplasia **2008**;10(12):1433-43.
30. Liu S, Cong Y, Wang D, Sun Y, Deng L, Liu Y*, et al.* Breast cancer stem cells transition between epithelial and mesenchymal states reflective of their normal counterparts. Stem Cell Reports **2014**;2:78-91 doi 10.1016/j.stemcr.2013.11.009.
31. Rolla S, Nicolo C, Malinarich S, Orsini M, Forni G, Cavallo F*, et al.* Distinct and non-overlapping T cell receptor repertoires expanded by DNA vaccination in wild-type and HER-

2 transgenic BALB/c mice. J Immunol **2006**;177(11):7626-33 doi 10.4049/jimmunol.177.11.7626

32. Tallerico R, Conti L, Lanzardo S, Sottile R, Wagner AK, Johansson MH*, et al.* NK cells control breast cancer and related cancer stem cell hematological spread. Oncoimmunology **2017**;6:1-11 doi 10.1080/2162402X.2017.1284718.

33. Li W, Ma H, Zhang J, Zhu L, Wang C, Yang Y. Unraveling the roles of CD44/CD24 and ALDH1 as cancer stem cell markers in tumorigenesis and metastasis. Scientific reports **2017**;7(1):13856 doi 10.1038/s41598-017-14364-2.

34. Harbeck N, Gnant M. Breast cancer. Lancet **2017**;389(10074):1134-50 doi 10.1016/S0140-6736(16)31891-8.

35. Hosseini H, Obradovic MM, Hoffmann M, Harper KL, Sosa MS, Werner-Klein M*, et al.* Early dissemination seeds metastasis in breast cancer. Nature **2016**;540(7634):552-8 doi 10.1038/nature20785.

36. Husemann Y, Geigl JB, Schubert F, Musiani P, Meyer M, Burghart E*, et al.* Systemic spread is an early step in breast cancer. Cancer cell **2008**;13(1):58-68 doi 10.1016/j.ccr.2007.12.003.

37. Quaglino E, Riccardo F, Macagno M, Bandini S, Cojoca R, Ercole E*, et al.* Chimeric DNA Vaccines against ErbB2+ Carcinomas: From Mice to Humans. Cancers **2011**;3(3):3225-41 doi 10.3390/cancers3033225.

38. Garg SK, Yan Z, Vitvitsky V, Banerjee R. Differential dependence on cysteine from transsulfuration versus transport during T cell activation. Antioxid Redox Signal **2011**;15(1):39-47 doi 10.1089/ars.2010.3496.

39. Arensman MD, Yang XS, Leahy DM, Toral-Barza L, Mileski M, Rosfjord EC*, et al.* Cystine-glutamate antiporter xCT deficiency suppresses tumor growth while preserving antitumor immunity. Proc Natl Acad Sci U S A **2019**;116(19):9533-42 doi 10.1073/pnas.1814932116.

40. Larocca C, Schlom J. Viral vector-based therapeutic cancer vaccines. Cancer journal **2011**;17(5):359-71 doi 10.1097/PPO.0b013e3182325e63.

41. Harper KL, Sosa MS, Entenberg D, Hosseini H, Cheung JF, Nobre R*, et al.* Mechanism of early dissemination and metastasis in Her2(+) mammary cancer. Nature **2016**;540:588–92 doi 10.1038/nature20609.

42. Chen RS, Song YM, Zhou ZY, Tong T, Li Y, Fu M*, et al.* Disruption of xCT inhibits cancer cell metastasis via the caveolin-1/beta-catenin pathway. Oncogene **2009**;28(4):599-609 doi 10.1038/onc.2008.414.

43. Korkaya H, Wicha MS. HER2 and breast cancer stem cells: more than meets the eye. Cancer Res **2013**;73(12):3489-93 doi 10.1158/0008-5472.CAN-13-0260.

44. Abravanel DL, Belka GK, Pan TC, Pant DK, Collins MA, Sterner CJ*, et al.* Notch promotes recurrence of dormant tumor cells following HER2/neu-targeted therapy. J Clin Invest **2015**;125(6):2484-96 doi 10.1172/JCI74883.
45. Osipo C, Patel P, Rizzo P, Clementz AG, Hao L, Golde TE*, et al.* ErbB-2 inhibition activates Notch-1 and sensitizes breast cancer cells to a gamma-secretase inhibitor. Oncogene **2008**;27(37):5019-32 doi 10.1038/onc.2008.149.
46. Lesniak D, Sabri S, Xu Y, Graham K, Bhatnagar P, Suresh M*, et al.* Spontaneous epithelial-mesenchymal transition and resistance to HER-2-targeted therapies in HER-2-positive luminal breast cancer. PLoS One **2013**;8(8):e71987 doi 10.1371/journal.pone.0071987.
47. Sato H, Shiiya A, Kimata M, Maebara K, Tamba M, Sakakura Y*, et al.* Redox imbalance in cystine/glutamate transporter-deficient mice. J Biol Chem **2005**;280(45):37423-9 doi 10.1074/jbc.M506439200.
48. Chintala S, Li W, Lamoreux ML, Ito S, Wakamatsu K, Sviderskaya EV*, et al.* Slc7a11 gene controls production of pheomelanin pigment and proliferation of cultured cells. Proc Natl Acad Sci U S A **2005**;102(31):10964-9 doi 10.1073/pnas.0502856102.
49. Damiao A, de Azevedo MFC, Carlos AS, Wada MY, Silva TVM, Feitosa FC. Conventional therapy for moderate to severe inflammatory bowel disease: A systematic literature review. World journal of gastroenterology **2019**;25(9):1142-57 doi 10.3748/wjg.v25.i9.1142.
50. Donofrio G, Cavirani S, Simone T, van Santen VL. Potential of bovine herpesvirus 4 as a gene delivery vector. Journal of virological methods **2002**;101(1-2):49-61 doi 10.1016/s0166-0934(01)00419-0

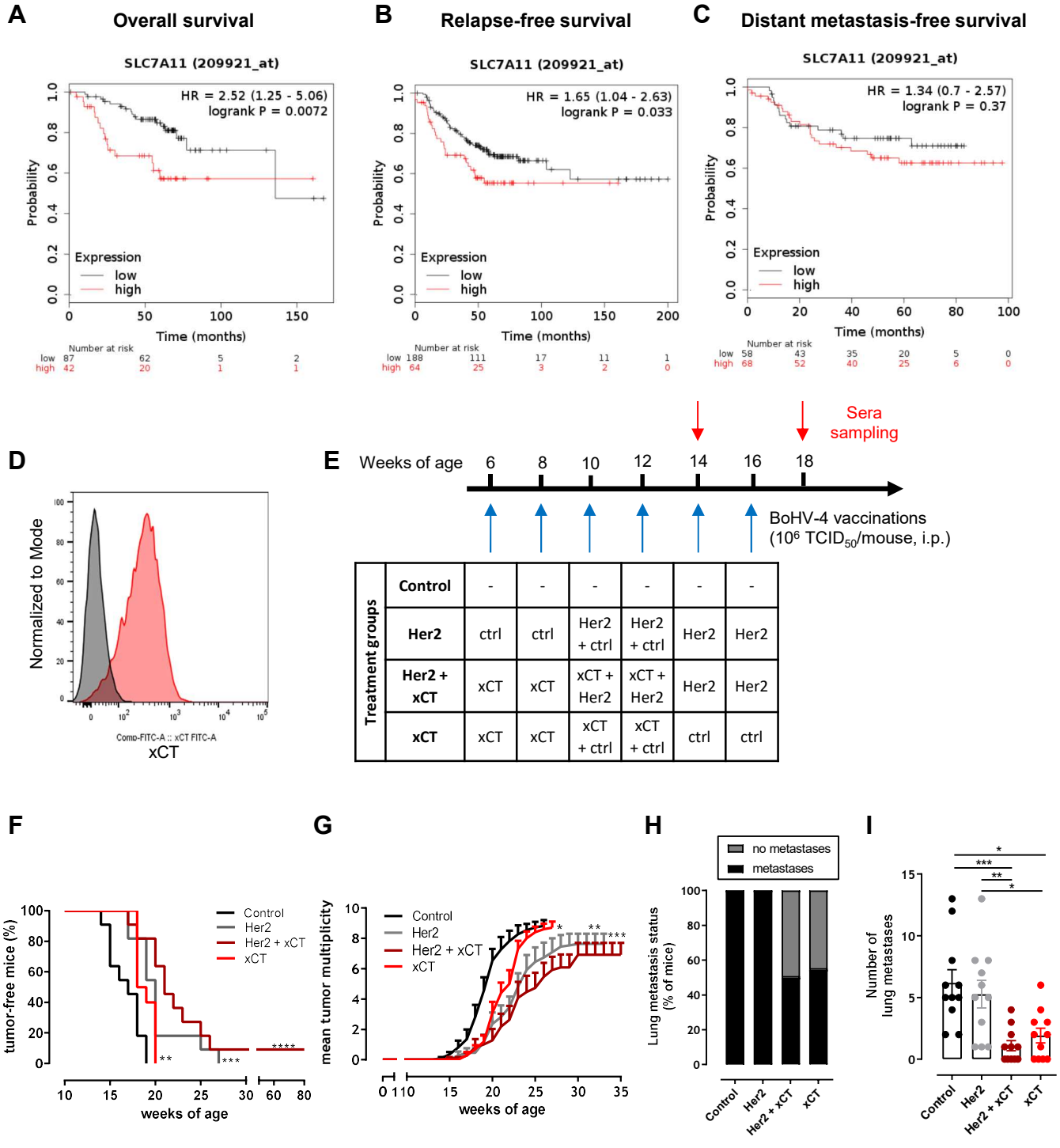

Figure 1. xCT is related to poor prognosis in Her2$^+$ breast cancer patients, and its immunotargeting potentiates anti-Her2 vaccination in BALB-neuT mice.

(A-C) Kaplan – Meier plots displaying overall **(A)**, relapse-free **(B)** and distant metastasis-free **(C)** survival in Her2$^+$ breast cancer patients stratified according to xCT mRNA expression. **(D)** Representative FACS analysis of xCT (red) or control Ab (grey) on a mammary tumor explanted from a BALB-neuT mouse. **(E)** Schematic representation of the immunization protocol of control BALB-neuT mice or mice vaccinated 6 times, every 2 weeks, with 10^6 $TCID_{50}$ of BoHV-4-ctrl and BoHV-4-Her2 (Her2); BoHV-4-xCT and BoHV-4-Her2 (Her2 + xCT); BoHV-4-xCT and BoHV-4-ctrl (xCT). (N=11 per group). **(F)** Tumor-free survival and **(G)** tumor multiplicity in control or immunized BALB-neuT mice. **(H)** Relative percentage of mice that developed (black) or not (grey) lung metastases. **(I)** Mean ± SEM of the number of superficial lung metastases observed in control or immunized mice. Each dot represents a single mouse. *, $P < 0.05$; **, $P < 0.01$, ***, $P < 0.001$; **(A-C, F)** Log-rank Mantel-Cox or **(G, I)** Student's *t* tests.

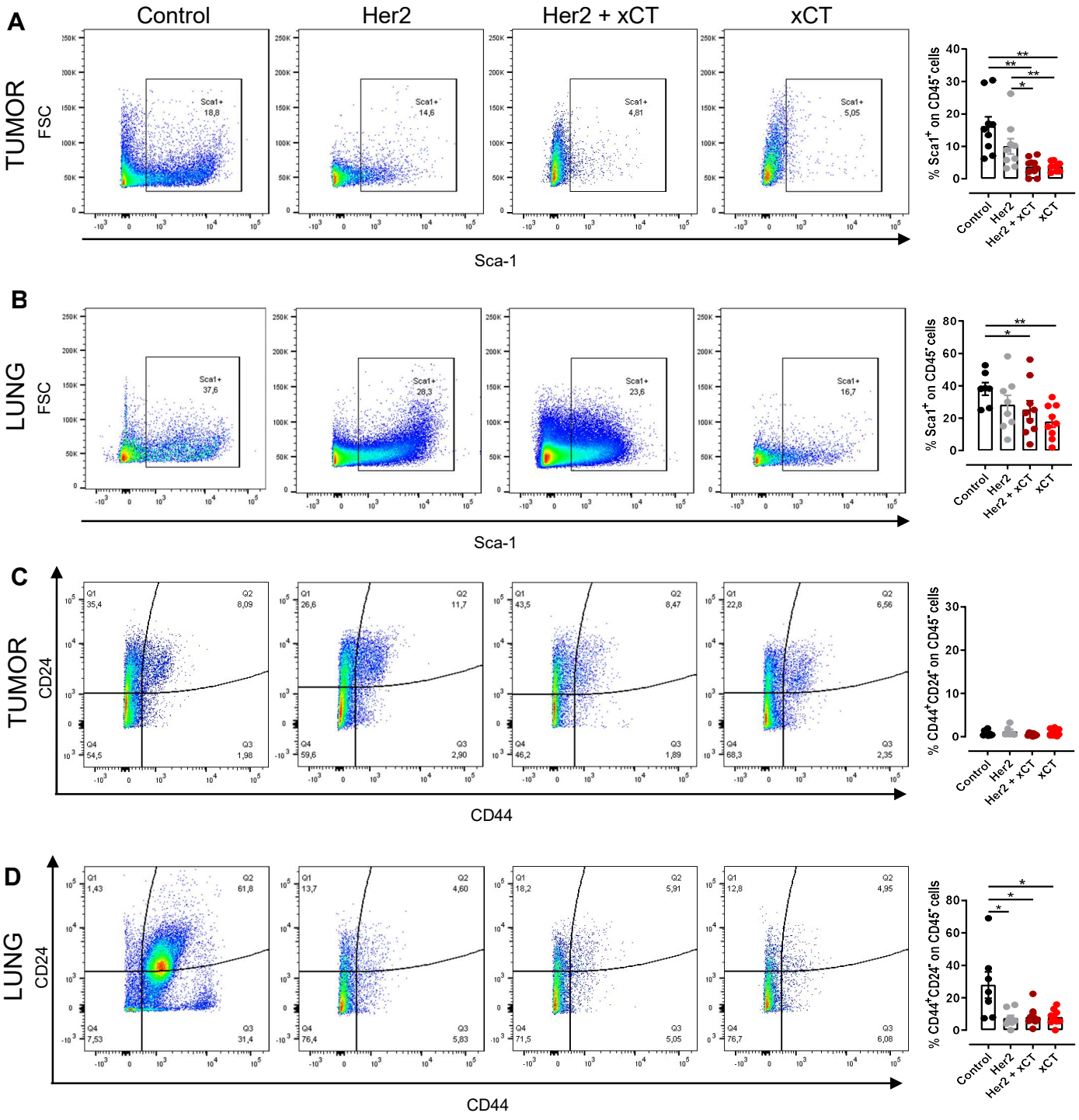

Figure 2. xCT immunotargeting decreases CSC frequency in BALB-neuT tumors and lungs. FACS analysis of **(A, B)** Sca1$^+$ and **(C, D)** CD44$^+$ CD24$^-$ CSC populations in **(A, C)** tumors and **(B, D)** lungs from control mice or mice treated with anti-Her2, anti-Her2 + anti-xCT, or anti-xCT vaccines. Representative dot plots and graphs showing the mean ± SEM of the percentage of CD45$^-$ cells expressing the CSC markers are shown. In graphs, each dot represents a single mouse. At least 6 mice per group were analyzed. *, $P < 0.05$; **, $P < 0.01$, Student's *t* test.

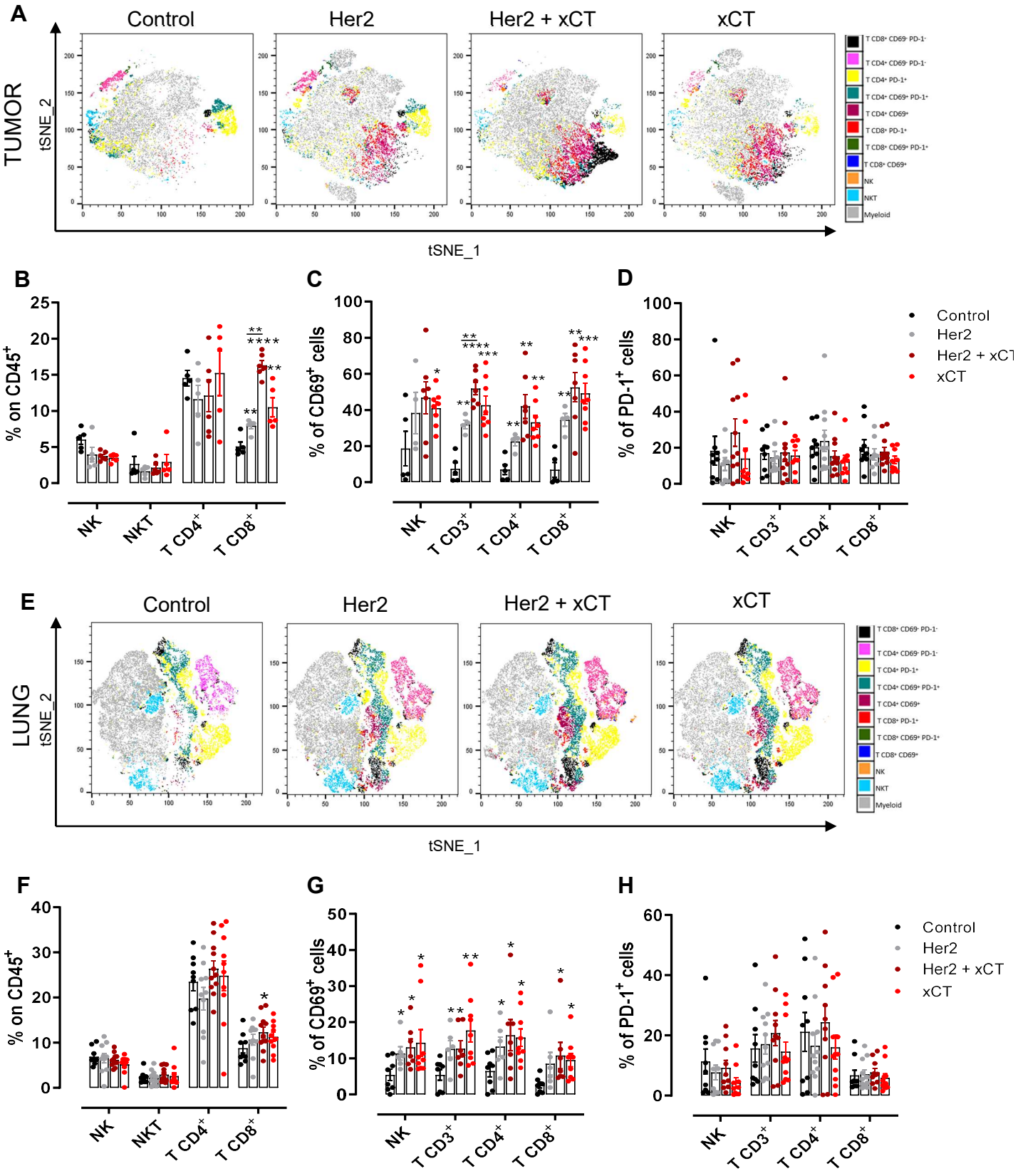

Figure 3. Her2 and xCT immunotargeting induces the activation of T lymphocytes in the tumors and lungs of vaccinated mice. FACS analysis of immune infiltrates in **(A-D)** tumors and **(E-H)** lungs of control BALB-neuT mice or mice immunized with anti-Her2, anti-Her2 + anti-xCT, or anti-xCT vaccines. **(A, E)** tSNE analysis run on 5000 live CD45$^+$ single cells per sample, on 5 samples per group. tSNE maps show concatenated FCS3 files for each group of mice, with the overlay of manually gated cell populations. **(B, F)** Graphs showing the percentage ± SEM of CD45$^+$ cells expressing the markers of NK (CD3$^-$ CD49b$^+$), NKT (CD3$^+$ CD49b$^+$), CD4$^+$ (CD3$^+$ CD49b$^-$ CD4$^+$) and CD8$^+$ (CD3$^+$ CD49b$^-$ CD8$^+$) T cell populations**.** Percentage ± SEM of **(C, G)** CD69$^+$ and **(D, H)** PD1$^+$ cells among T and NK cell populations. Each dot represents a single mouse. *, $P < 0.05$; **, $P < 0.01$, ***, $P < 0.001$, Student's t test.

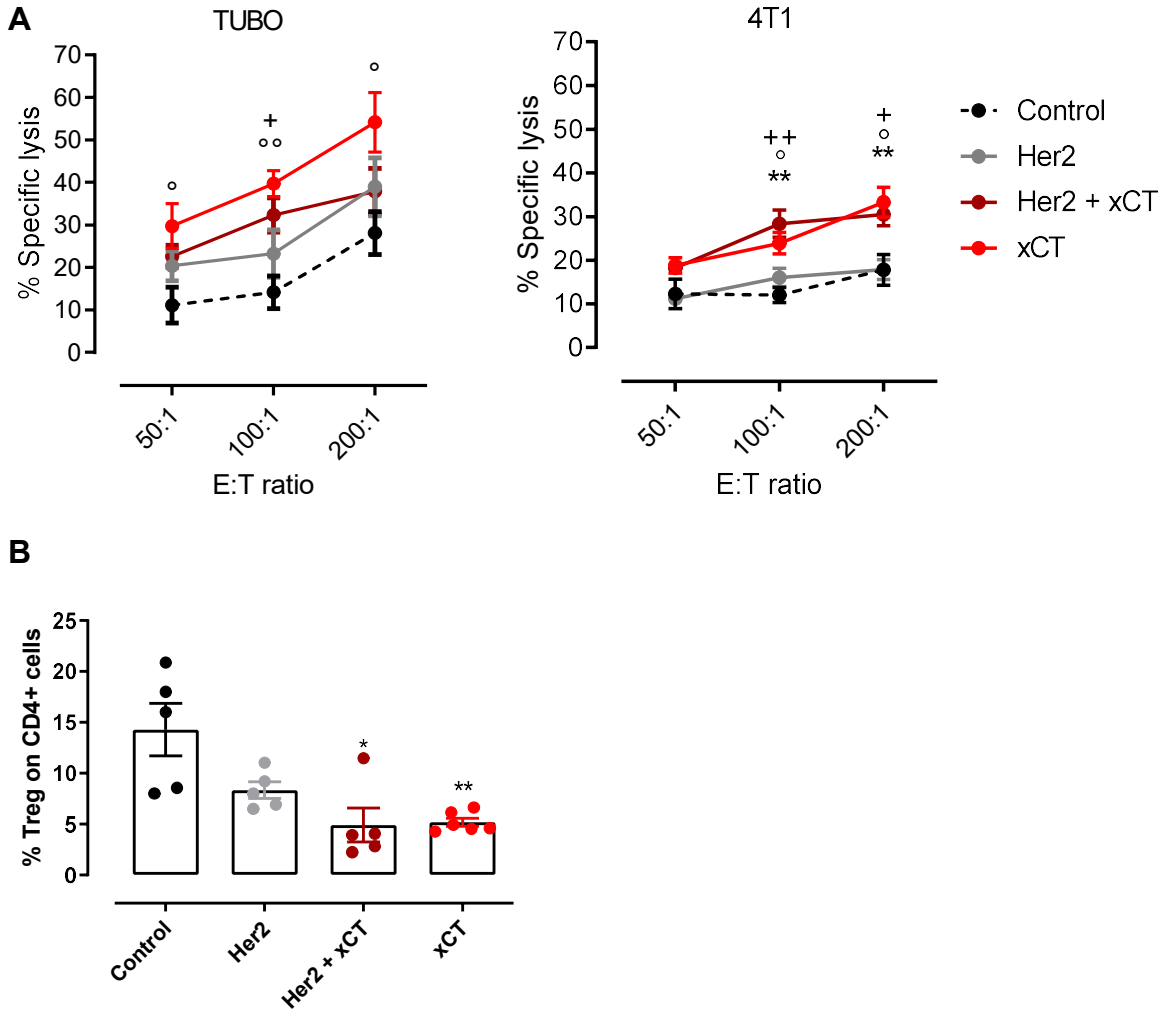

Figure 4. Anti-xCT vaccination induces T cell cytotoxicity of xCT$^+$ breast cancer cells and decreases circulating Treg cells. (A) SPC from control or vaccinated mice (N=4 per group) were co-cultured at different E:T ratios (200, 100 or 50:1) with CFSE$^+$ TUBO or 4T1 cells for 48 h. The percentage of 7-AAD$^+$ dead cells among CFSE$^+$ cells was analyzed by FACS. Graphs show means ± SEM of the percentages of specific lysis. *, $P < 0.05$, **, $P < 0.01$: Her2 + xCT vs Her2 or control. °, $P < 0.05$, °°, $P < 0.01$: xCT vs Her2 or control. $^+$, $P < 0.05$; $^{++}$, $P < 0.01$, Her2 vs control; Student's *t*-test. **(B)** Means ± SEM of the percentage of Tregs (CD3$^+$ CD4$^+$ CD25^{high} GITR$^+$ Foxp3$^+$) among CD4$^+$ T lymphocytes analyzed at sacrifice in the peripheral blood of BALB-neuT mice (N ≥ 5 mice per group) Each dot represents a single mouse. *, $P < 0.05$; **, $P < 0.01$, Student's *t*-test.

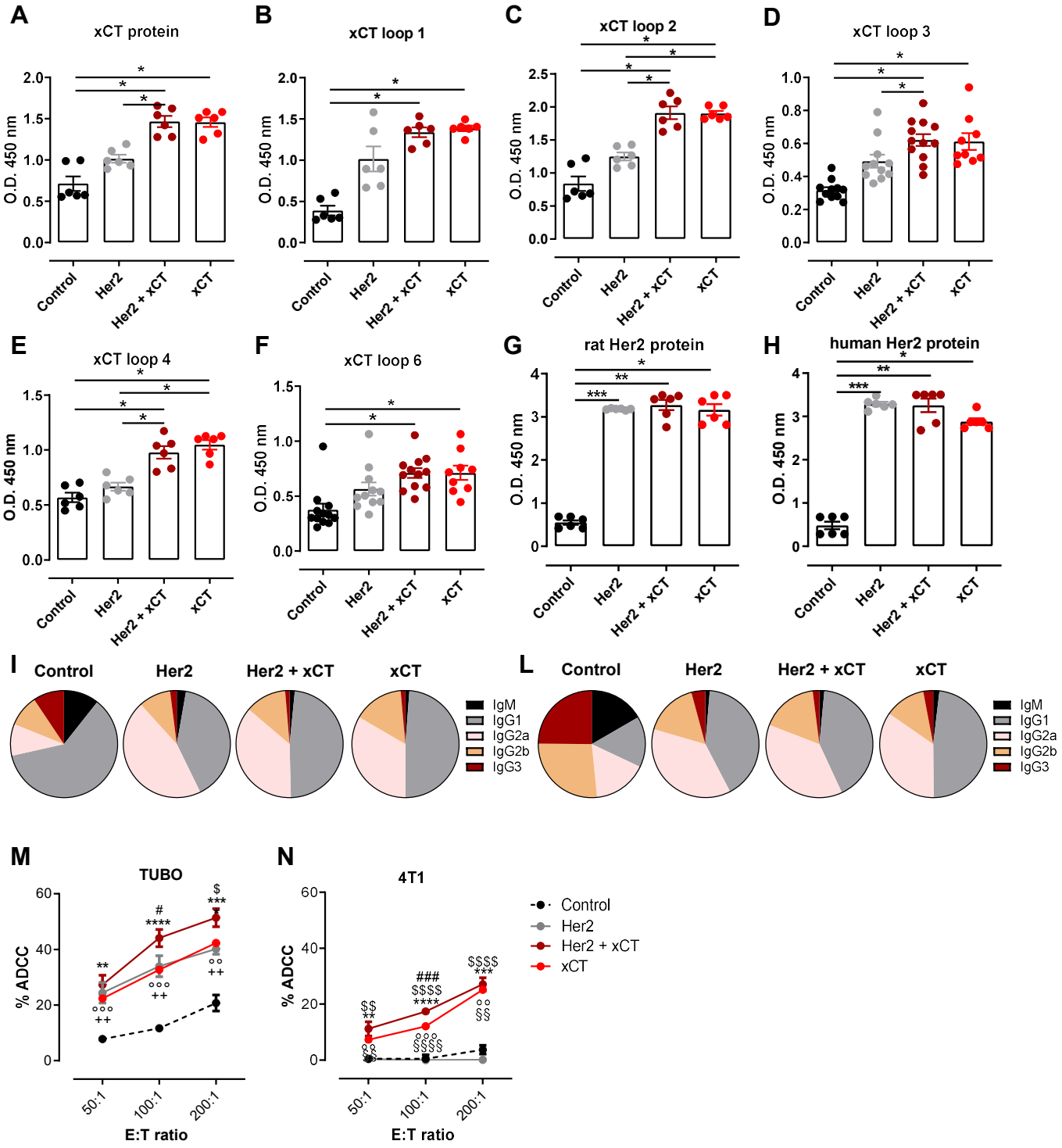

Figure 5. xCT and Her2 immunotargeting induces specific humoral responses that induce ADCC. Pooled sera from control or vaccinated BALB-neuT mice were tested by ELISA on **(A)** mouse xCT protein; peptides representing mouse xCT extracellular loops **(B)** 1, **(C)** 2, **(D)** 3, **(E)** 4 or **(F)** 6; the recombinant extracellular domains of **(G)** rat or **(H)** human Her2 proteins. Graphs show means ± SEM of two pools analyzed from 3 independent experiments. *, $P < 0.05$; **, $P < 0.01$, ***, $P < 0.001$, Student's *t* test. **(I, L)** Proportion of **(I)** anti-xCT and **(L)** anti-Her2 Ig isotypes analyzed by ELISA in the sera of control or vaccinated mice. **(M, N)** ADCC analyzed *in vitro* on $CFSE^+$ **(M)** TUBO or **(N)** 4T1 target cells incubated with a 1:50 dilution of sera pooled from control or vaccinated mice and SPC from naive mice at different E:T ratios (200, 100, and 50:1). Results shown are the mean ± SEM of the percentage of ADCC. Statistical analysis was performed with Student's *t* test as follows; $^+$, Control vs Her2. *, Control vs Her2 + xCT. °, Control vs xCT. $^\$$, Her2 vs Her2 + xCT. §, xCT vs Her2 + xCT. #, xCT vs Her2 + xCT. 1 symbol, $P < 0.05$; 2 symbols, $P < 0.01$; 3 symbols, $P < 0.001$; 4 symbols, $P < 0.0001$.

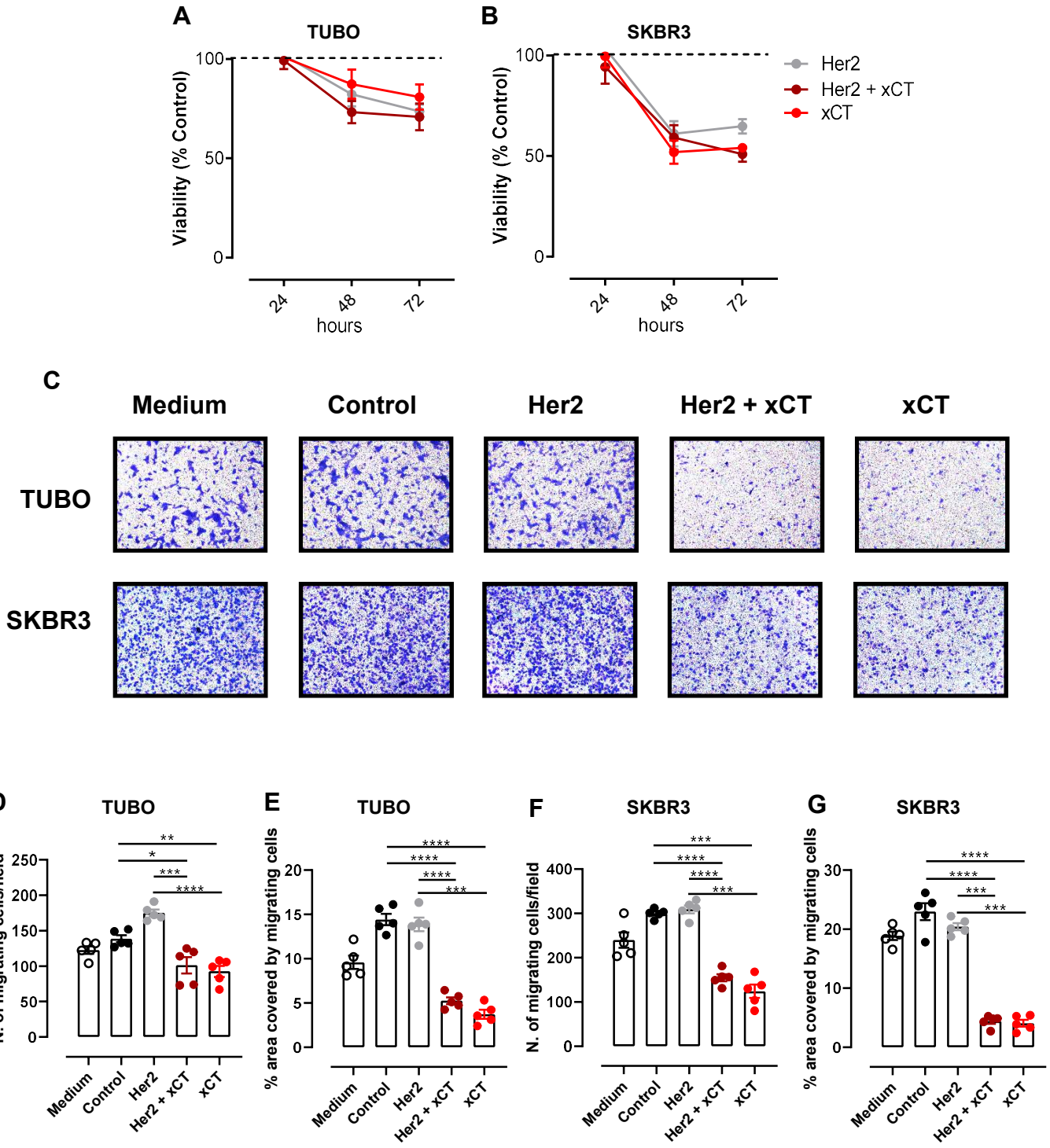

Figure 6. Anti-Her2 and anti-xCT antibodies differentially impair cancer cell viability and migration. MTT analysis of cell viability of **(A)** TUBO and **(B)** SKBR3 cells incubated for 24, 48 and 72 h with a 1:50 dilution of sera pooled from control or vaccinated BALB-neuT mice. Results are shown as means ± SEM of the percentage of cell viability compared to cells incubated with control sera, from 3 independent experiments. **(C-G)** Effect of sera on cell migration assessed using the Transwell migration assay on TUBO and SKBR3 cells. **(C)** Representative images of cells migrated to the lower surface of the transwell filter and stained with crystal violet. Graphs show the means ± SEM of **(D, F)** the number of migrated cells and **(E, G)** the % of area covered by migrated cells, counted in five different fields. A representative experiment out of three is shown. *, $P < 0.05$; **, $P < 0.01$, ***, $P < 0.001$; ****, $P < 0.0001$, Student's *t* tests.

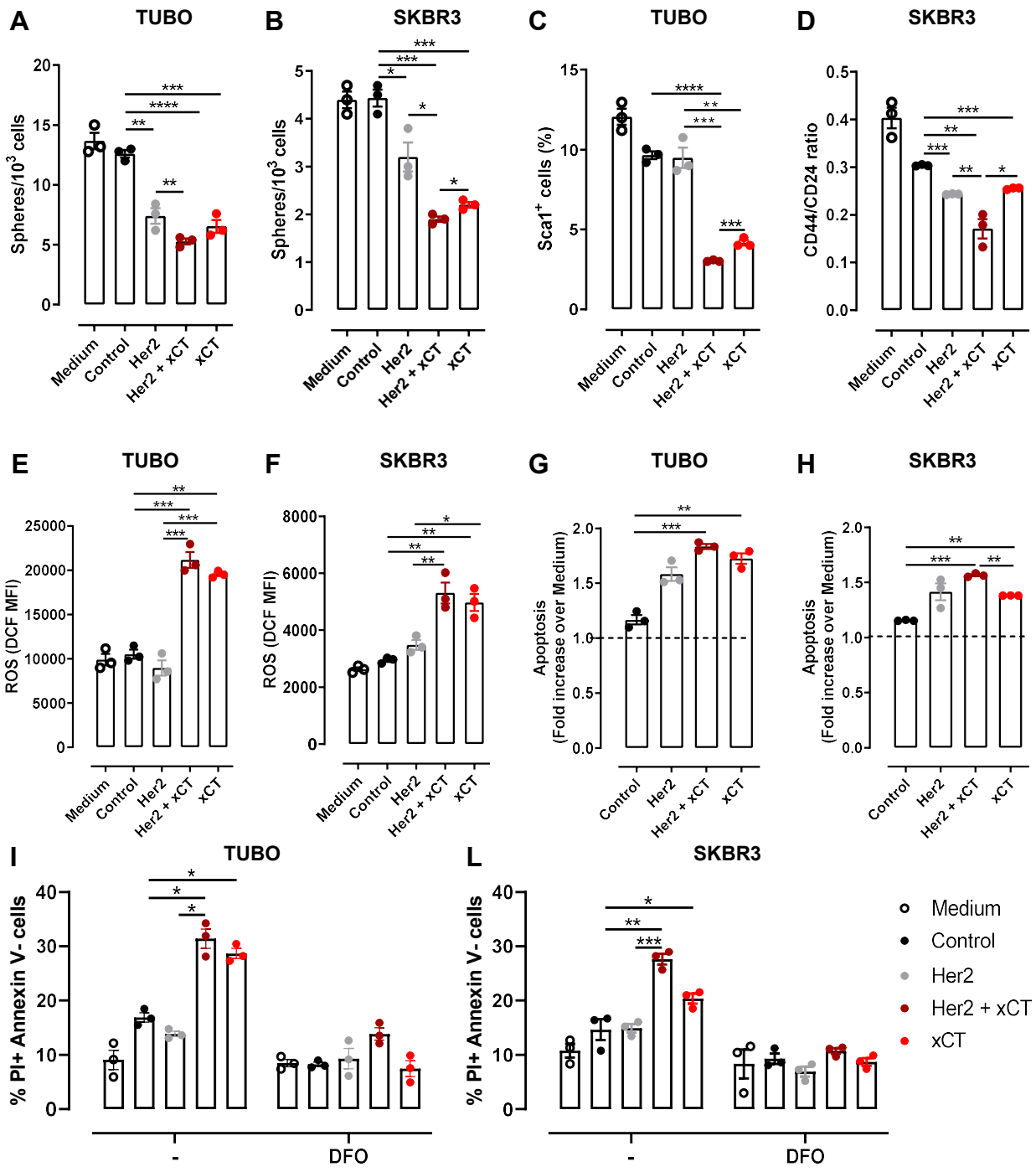

Figure 7. Vaccination-induced anti-xCT antibodies target CSCs by increasing ROS, apoptosis and ferroptosis. (A-H) Cells dissociated from tumorspheres generated from TUBO or SKBR3 cells were incubated for 5 days with medium, or with a 1:50 dilution of sera pooled from control or vaccinated mice. **(A, B)** Sphere generating ability reported as number of second passage tumorspheres generated every 10^3 plated cells. **(C)** Means ± SEM of the percentage of $Sca1^+$ cells analyzed by FACS in TUBO tumorspheres. **(D)** Means ± SEM of the ratio between the percentage of $CD44^+$ and $CD24^-$ cells quantified by FACS in SKBR3 tumorspheres. **(E, F)** FACS analysis of intracellular ROS content, reported as means ± SEM of DCF MFI. **(G-H)** FACS analysis of apoptosis, reported as mean ± SEM of the fold increase of Annexin V^+ cells compared to tumorspheres cultured in medium alone. **(I-L)** Analysis of ferroptosis in cells dissociated from tumorspheres generated from TUBO or SKBR3 cells and incubated for 24 h with medium, or with sera from control or vaccinated mice (1:50), in the absence or presence of the iron chelator DFO (50 μM). Means ± SEM of the percentage of Annexin V^-/propidium iodide $(PI)^+$ cells is reported. Each dot represents an independent experiment. *, $P < 0.05$; **, $P < 0.01$, ***, $P < 0.001$, ****, $P < 0.0001$, Student's *t* test.